Chem.Phys. Lett. 314 (1999) 195-202

Adsorption of Water on FeO(111) and Fe_3O_4(111): Identification of Active Sites for Dissociation

Y. Joseph, C. Kuhrs, W. Ranke*, M. Ritter and W. Weiss

Department of Inorganic Chemistry, Fritz-Haber-Institute of the MPG, Faradayweg 4-6, 14195 Berlin, Germany

* Corresponding author: e-mail ranke@fhi-berlin.mpg.de, phone +49 30 8413 4523, fax +49 30 8413 4621

Accepted 1999

Abstract

The adsorption of water on epitaxial FeO(111) and Fe_3O_4(111) films structurally well characterized by STM and LEED was investigated with photoelectron and thermal desorption spectroscopy. On the FeO(111) surface terminated by a close-packed oxygen layer monomeric water species get physisorbed. On the Fe_3O_4(111) surface terminated by ¼ monolayer of Fe atoms located over a close-packed oxygen layer underneath water dissociates resulting in adsorbed OH groups. The OH saturation coverage corresponds to the number of surface Fe atoms, which is much larger than the surface defect concentrations. Therefore, the dissociation takes place at Fe sites exposed on the regular Fe_3O_4(111) surface, and the FeO(111) surface is chemically inert because no Fe sites exist thereon.

Keywords:

Introduction

The interaction of water with metal-oxide surfaces plays an important role in fields like heterogeneous catalysis, electrochemistry, environmental science and corrosion. Water can adsorb molecularly or dissociatively, the latter usually results in adsorbed hydroxyl groups on the surface. Many polycrystalline oxide materials used as catalysts or catalyst supports get hydroxilated in the presence of water vapor as a result of dissociative adsorption, like for example silica, Al_2O_3 [1], and zeolithes [2], and their catalytic properties can get strongly altered by this hydroxilation. For metal surfaces a detailed picture of the dissociation process has evolved [3]. Here, the thermodynamic driving force is the formation of stable metal-oxygen or metal-hydroxyl bonds. The large O-H bond dissociation energy of the free water molecule (498 kJ/mol) gets reduced by the formation of a transition state with a metal-oxygen bond between the substrate and the water adsorbate, which weakens one O-H bond within the water molecule resulting in the dissociation. In case of metal oxides, insight into the role of atomic surface structural elements for the water adsorption process has evolved from many theoretical and experimental studies performed on metal-oxide single crystals or thin epitaxial films. For NiO(100), Cr_2O_3(111) [4] and TiO_2(110) [5] it was clearly shown that dissociative adsorption of water only takes place at defects and not at regular surface sites. No clear picture still has evolved for the Fe_2O_3(0001) surface [6-8] and many other surfaces, where dissociation seems to take place on regular surface areas as well as at defect sites. On Al_2O_3(0001) single crystal surfaces terminated by Al atoms [9] water dissociates on the regular surface areas [10], whereas thin epitaxial films terminated by O atoms are chemically inert [11]. A comparative study over Zn-rich (001) and O-rich (001) faces of ZnO single crystals revealed a higher reactivity for the Zn-rich face [12]. These results indicate that chemical reactivity of metal-oxides is related to exposed metal sites. However, in most of these studies the atomic surface structures and surface defect concentrations were not known precisely, which is important in order to unequivocally elucidate the structural elements that are involved in the dissociative adsorption.

The interaction of water with iron oxides plays an important role in several heterogeneous catalytic reactions, like the water-gas shift reaction [13] and the dehydrogenation of ethylbenzene to styrene [14]. It also is of high inter-

est regarding the photocatalytic splitting of water, which can be performed over iron oxide electrodes [15]. We studied the adsorption of water on structurally well characterized FeO(111) surfaces exposing only O atoms and on Fe_3O_4(111) surfaces exposing both Fe and O atoms. Only on Fe_3O_4(111) a dissociative adsorption resulting in adsorbed OH species is observed, and it is shown that the dissociation is not related to defects but predominantly takes place on regular surface areas of this oxide. This comparative study demonstrates that the dissociation is related to the Fe atoms exposed on the surface. It is proposed that the OH group is bound to the surface Fe atoms and the H species to neighboring O sites, as predicted by recent simulations for the dissociative adsorption of H_2O on the Al-terminated Al_2O_3(0001) surface [16].

Experimental

The experiments were performed in several ultrahigh vacuum systems with base pressures below 10^{-10} mbar and equipped with standard facilites for sample cleaning. The Pt(111) substrate crystal was 2 mm thick and had a diameter of 10 mm. It could be heated by electron bombardment from the back and cooled by a liquid nitrogen reservoir, the sample temperature was measured with a chromel-alumel thermocouple spotwelded to the edge of the crystal. The photoelectron spectroscopy chamber was equipped with a high resolution spot-profile low energy electron diffraction (LEED) system, a double-pass cylindrical mirror analyser and a He resonance lamp. The UPS measurements were performed under conditions of dynamic adsorption-desorption equilibrium. A constant water vapor pressure is established in the chamber and the spectra were taken at different sample temperatures after the corresponding equilibrium coverages were reached, which took up to 6 minutes. As described in detail in ref. [17] difference spectra are obtained by subtracting the clean surface spectrum attenuated by a factor AF from the adsorbate covered surface spectrum. The attenuation factor AF is determined in a spectral region where no adsorbate emission exists and the substrate emission is not visibly affected, which is about 0.5 eV below the Fermi level. It allows to determine the relative adsorbate coverage according to the Lambert-Beer absorption law [18] and to estimate the absolute coverage Θ using tabulated electron mean free paths [19]. Also the integrated total intensity of adsorbate emission in the spectra gives a coverage scale. Both scales agree very good. The scanning tunneling microscopy (STM) and thermal desorption spectroscopy (TDS) measurements were performed in two different chambers both equipped with backview LEED systems and Auger electron spectrometers as described in detail in ref. [20]. STM images were obtained with electrochemically etched tungsten tips in the constant current mode. The TDS measurements were performed with a heating rate of 5 K/sec after exposing the samples to water at T=100 K or 200 K. A calibration experiment was performed in order to convert the H_2O TDS signals into a hydroxyl coverage in terms of OH groups/cm^2. For this, thick ice films were grown onto the samples at T=100 K at a known H_2O background pressure measured with an ionization gauge. A linear increase of the TDS peak area corresponding to the condensed ice multilayers, which is labeled α in Fig. 2, was obtained as a function of exposure (which was extended up to 60 L). Since the sticking and condensation coefficient for H_2O on an ice multilayer are both unity for temperatures below 150 K [21], the number of adsorbed water molecules per cm^2 can be calculated from the H_2O exposure, and this number can be attributed to the TDS peak area measured in the corresponding desorption run. In order to exclude temporal changes of the mass spectrometer sensitivity this calibration experiment was done immediately after the TDS measurements on Fe_3O_4(111). Epitaxial FeO(111) and Fe_3O_4(111) films were grown onto the Pt(111) substrate by repeated cycles of iron deposition at room temperature and subsequent oxidation at temperatures between 870 and 1000 K in 10^{-6} mbar oxygen. The exact preparation procedure is described in detail in ref. [22].

Results and Discussion

Fig. 1a displays 55×55 $Å^2$ STM images of an FeO(111) monolayer film (a) and an Fe_3O_4(111) film more than 100 Å thick (b). In the lower parts, schematic top view representations of the corresponding surface structures are shown. The FeO(111) film in (a) completely wets the platinum substrate and exhibits a hexagonal lattice of protrusions with a 3.1 Å periodicity. Electron-scattering quantum-chemistry calculations performed for this film revealed the protrusions to correspond to surface O atom positions [23]. It consists of a hexagonal close-packed Fe-O bilayer terminated by an outermost oxygen layer as depicted schematically in Fig. 1a, which also was deduced from photoelectron diffraction experiments [24]. The large moiré superstructure in the STM image is caused by the lattice mismatch to the substrate surface lattice and creates the satellite spots in the LEED pattern of this film depicted in the insert of Fig. 2a. With X-ray photoelectron spectroscopy an Fe2p core level binding energy corresponding to Fe^{2+} was observed [25], indicating an ionic character of the Fe-O bond in this ultrathin film. The FeO(111) film grows layer-by-layer up to a thickness of about 2.5 bilayers, where the second and third layers exhibit very similar STM images [26].

The STM image of the Fe_3O_4(111) surface shown in Fig. 1b exhibits a hexagonal lattice of protrusions with a 6 Å periodicity, which corresponds to the LEED pattern of this film depicted in the insert of Fig. 2b. As determined in a previous LEED analysis this surface exposes ¼ ML of Fe atoms over a close-packed oxygen layer underneath [27]. Here, the protrusions in the STM image correspond to the positions of the topmost layer Fe atoms. This assignment agrees with spin-density functional theory calculations that revealed the dominant electron density of states near the Fermi level to be related to Fe3d states of these Fe atoms [28]. The missing protrusions represent the dominant type of

point defects on these surfaces and are assigned to Fe vacancies. The maximal concentration of Fe vacancies we observed on these films was 30 %, most films exhibit vacancy concentrations around 10%. We always observe steps 4.8 Å or multiples thereof high, which corresponds to the distance between equivalent Fe_3O_4(111) surface terminations. Typical step separations observed by STM are 200-500 Å, which agrees well with the LEED spot broadening measured at out-of-phase scattering conditions for monoatomic steps 4.8 Å high.

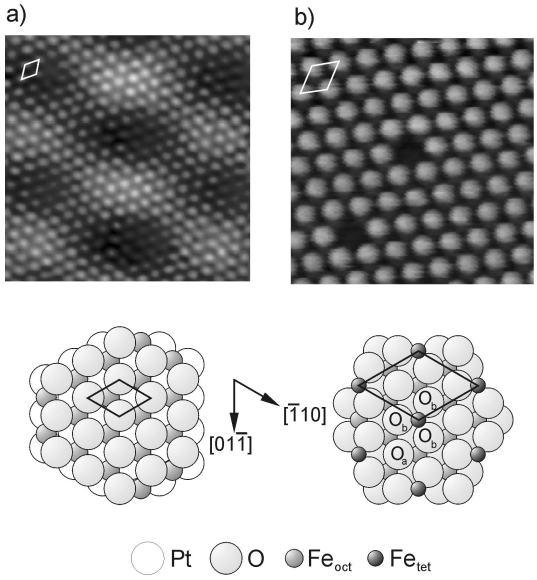

Figure 1: 55×55 Å^2 STM images of the FeO(111) monolayer (a) and Fe_3O_4(111) multilayer surfaces (b). Below schematic top view representations of the corresponding surface structures are shown. Fe atoms octahedrally (Fe_{oct}) and tetrahedrally (Fe_{tet}) coordinated in the bulk oxides and the surface unit cells are indicated. All atoms are drawn in their full ionic sizes. O_a and O_b denote symmetrically inequivalent oxygen atoms on Fe_3O_4(111). In the STM images the protrusions correspond to surface oxygen atoms in case of FeO(111) (a) and to surface Fe atoms in case of Fe_3O_4(111) (b). The large moiré superstructure in (a) is caused by the lattice mismatch to the Pt(111) substrate. (a) U_T = 0.9 V, I_T= 0.3 nA, (b) U_t=-0.9 V, I_t=0.5 nA.

Fig. 2 shows thermal desorption spectra of water adsorbed onto the two iron oxide surfaces. On FeO(111), a desorption maximum at T=170 K is observed for the lowest exposure, which is attributed to physisorbed water labeled β desorbing with a first order kinetics. It initially shifts to 165 K, for exposures above 0.6 Langmuir (L) the desorption traces exhibit a common leading edge and no saturation occurs with further increasing exposure. These signals are due to zero order desorption of condensed ice multilayers labeled α. On the Fe_3O_4(111) surface a desorption maximum around 280 K evolves for the lowest exposures, which shifts to 265 K with increasing exposure. It is attributed to chemisorbed water species labeled γ, which desorb with a second order kinetics as indicated by the symmetrical shape and the temperature shift of the desorption maximum. After saturation of this chemisorption signal a second desorption maximum shifting from 215 to 185 K evolves. It saturates at around 2 L and is attributed to first order desorption of pysisorbed water species labeled β. Finally, zero order desorption of condensed ice multilayers labeled α is observed.

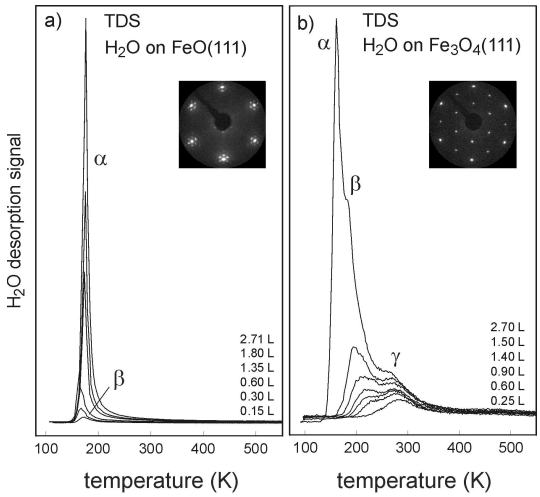

Figure 2: Thermal desorption traces of water after adsorption onto FeO(111) (a) and Fe_3O_4(111) (b) at T=100 K. Exposures are indicated in Langmuir units. The inserts show LEED patterns of the respective clean oxide films for an electron energy of E=60 eV.

The upper curve in Fig. 3 shows the UP valence band difference spectrum of the saturated physisorbed water layer on FeO(111), which is formed at a sample temperature of 155 K and a vapor pressure of $p(H_2O)=10^{-8}$ mbar. The binding energy is referenced to the vacuum level E_{VAC}, and the orbital energy positions for gas phase water are indicated by the bars. The spectrum exhibits three peaks that are attributed to emission from the $1b_1$, $3a_1$ and $1b_2$ orbitals of molecular water. The energy separations between these peaks are identical to those of gaseous water [29], they only are shifted by a relaxation shift of ΔE_R =1.8 eV to lower binding energies. Also the shape of the spectrum agrees well with gas phase spectra of water [29]. Since for hydrogen bonded water molecules different orbital energy separations and spectral shapes due to splitted or broadened molecular orbitals would be expected [30], we conclude that monomeric water species are adsorbed. The work function decreases by 0.83 eV upon saturation of this monomeric water layer, as deduced from the shift of the low energy onset of the UP spectrum. With further increasing water coverage a hydrogen bonded water bilayer is formed, followed by the condensation of ice multilayers [18]. From the UPS attenuation factor AF and the TDS signals a saturation coverage around 4×10^{14} molecules cm^{-2} can be estimated for the monomeric water layer, which would correspond to the density of an $(\sqrt{3}\times\sqrt{3})R30°$ adsorbate layer with respect to the FeO(111)-(1×1) surface lattice. The initial dipole moment of one adsorbed water molecule is calculated to be about 1.5 D, only slightly smaller than that of the free water molecule (1.8 D). Based on these results we conclude that monomeric water

molecules adsorb in an upright or slightly tilted geometry with their oxygen atoms oriented towards the substrate, as observed on most metal surfaces [3].

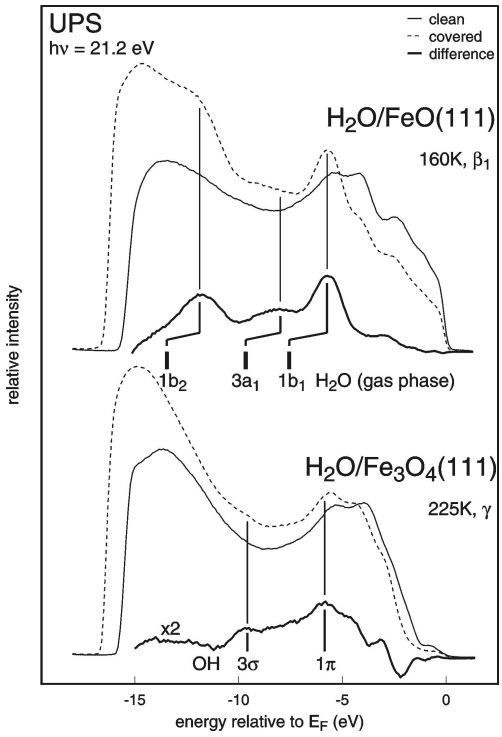

Figure 3: UP valence band spectra of the clean oxide surfaces, after saturation of the species adsorbing first upon water exposure, as well as background corrected difference spectra. On FeO(111) monomeric water adsorbs first, whereas dissociatively adsorbed water is found on Fe_3O_4(111). The spectra were measured at a constant vapor pressures $p(H_2O)=1x10^{-8}$mbar and at the indicated sample temperatures. The energy positions of the molecular orbitals of gaseous water (shifted by the work function of 5.04 eV) and of the OH groups are indicated.

The lower curve in Fig. 3 shows the UP valence band difference spectrum of the saturated chemisorbed water layer on Fe_3O_4(111), obtained at 225 K and a vapor pressure of $p(H_2O)=10^{-8}$ mbar. Two main peaks can be seen here, which are attributed to emission from the 1π and 3σ orbitals of adsorbed OH groups. Similar spectra were observed for free OH radicals [31] and for OH groups adsorbed on other metal-oxides [32]. The features between -5 and -10 eV below E_{VAC} are probably due to adsorbate induced changes of the substrate emission and to emission from the coadsorbed hydrogen species. The presence of OH groups is also evident from X-ray photoelectron spectroscopy measurements (XPS), where a shoulder on the high binding energy side of the Fe_3O_4(111) substrate O1s core level is observed. A curve fitting procedure reveals this shoulder to correspond to a second signal with a chemical shift of 2.1 eV, which is characteristic for OH groups. The dissociative adsorption of water into OH+H is further indicated by the second order desorption kinetics deduced from the TDS traces in Fig. 2b and from adsorption isobars measured by UPS under adsorption-desorption equilibrium conditions as discussed in detail in ref. [18]. From the TDS peak area of the saturated γ signal in Fig. 2b a saturation coverage of 2×10^{14} molecules cm^{-2} is obtained, which agrees well with the OH coverages deduced from the UPS attenuation factor AF and from the integrated area of the OH induced O1s signal measured by XPS [18]. This saturation coverage corresponds to about one OH+H per Fe atom exposed on the regular Fe_3O_4(111) surface, which is much higher than the atomic defect concentrations deduced from the STM and LEED investigations discussed above. Therefore, the dissociation of water on Fe_3O_4(111) is not related to defects but takes place predominantly on regular surface areas. Indeed, we find lower OH saturation coverages on surfaces with higher defect concentrations [18]. In agreement with the TDS data in Fig. 2b we observe coadsorbed monomeric β-water after saturation of the chemisorbed OH γ–species as the coverage increases, followed by final condensation of α-ice multilayers. Detailed adsorption models for the adsorbed water species observed on the FeO(111) and Fe_3O_4(111) surfaces and their adsorption thermodynamics are presented elsewhere [18].

Summary and conclusions

A physisorption of water monomers is observed on the O-terminated FeO(111) surface. So far there exists very few experimental evidence for monomeric water species that remain stable after adsorption, one example is H_2O on Pt(111) [33]. Usually, adsorbed water monomers are very mobile and immediately form hydrogen bonded clusters [3]. From the work function decrease observed here we conclude that the water molecules are adsorbed with their oxygen atoms oriented towards the substrate surface. This unexpected adsorption geometry must be favored by the strongly reduced Fe-O interlayer spacing in the FeO(111) film, which is accompanied by a lateral lattice expansion [24,26]. We propose that electric field lines pointing into the Fe cations located in the second layer penetrate through the hollow sites of the outermost oxygen layer, where they add constructively with the electric field lines emerging from the oxygen atoms of the adsorbed water molecules. This leads to an attractive electrostatic interaction. Such a mechanism was proposed recently to account for the attractive interactions measured between hydrophilic surfaces in liquid water using the surface force apparatus, where for the smallest distances two adsorbed water layers are confined between the two surfaces with their oxygen atoms pointing towards each other [34]. A flat lying adsorption geometry as observed for water on MgO(100) [35] with a dipole moment induced only by polarization seems unlikely when considering the large dipole moment observed here.

In contrast to FeO(111), a dissociative adsorption resulting in adsorbed OH species is observed on the Fe_3O_4(111) surface terminated by ¼ ML of Fe atoms. Since the OH saturation coverage roughly corresponds to the number of Fe atoms exposed on this surface, which is much higher than the surface defect concentration, the dissociation predominantly takes place on regular Fe_3O_4(111) surface

areas. A comparison of the FeO(111) and Fe_3O_4(111) surface structures proofs that the dissociation reaction is directly related to Fe atoms exposed on the latter surface. We propose the reaction mechanism depicted schematically in Fig. 4. In the first step the water molecule is adsorbed associatively via its oxygen lone pair orbital onto an Fe site exposed on the surface (a). Here, the coordinatively unsaturated Fe site acts as a Lewis acid that attracts the lone pair electrons of the water molecule. A mixing between substrate Fe3d and O2p states of water can lead to a substrate-adsorbate bond that weakens the OH bonds within the water molecule, thereby reducing the OH bond dissociation energy. After the dissociation took place the resulting OH^- group remains adsorbed at the Fe site and the H^+ species is adsorbed onto an neighboring O site, as depicted in Fig. 4b. This heterolytic dissociation might also be considered as an acid-base reaction, where the coordinatively unsaturated Fe and O sites act as Lewis acids and Broensted bases, respectively. As can be seen in Fig 4, on the Fe_3O_4(111) surface the Fe cations and neighboring basic O anions are located in a distance that fits to the geometry of the water molecule quiet well, which allows the dissociation to occur in an effective manner.

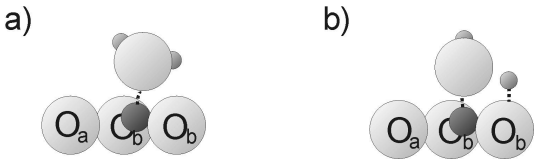

Figure 4: Schematic side view representation of a water molecule associatively adsorbed via its oxygen atom onto an Fe site exposed on Fe_3O_4(111) (a). In (b) adsorbed OH^- and H^+ species resulting from heterolytic dissociation of the water molecule are depicted. The Fe_3O_4(111) surface atoms are drawn in their full ionic sizes, their positions were taken from a recent LEED crystallography surface structure determination [27] without considering adsorbate induced relaxations.

Acknowledgements

The authors are obliged to R. Schlögl for support and stimulating discussions. The work was supported in part by the Deutsche Forschungsgemeinschaft.

References

[1] H. Knözinger in *"The Hydrogen Bond"*, Vol. 3, pp. 1263-1364, Eds.: P. Schuster, G. Zundel and C. Sandorfy, North-Holland, Amsterdam (1976).

[2] J.W. Ward, in: Zheolite Chemistry and Catalysis, Ed: J.A. Rabo, p. 118, Am. Chem. Soc., Washington, D.C. 1976.

[3] P.A. Thiel and T.E. Madey; Surf. Sci. Rep. 7 (1987) 211.

[4] D. Cappus, C. Xu, D. Ehrlich, B. Dillmann, C.A. Ventrice, K. Al Shamery, H. Kuhlenbeck, and H.-J. Freund; Chem. Phys. 177 (1993) 533.

[5] M.A. Henderson, Surf. Sci. **355** (1996) 151.

[6] M. Hendewerk, M. Salmeron, and G.A. Somorjai; Surface Science **172**, 544 (1986)

[7] R.L. Kurtz and V.E. Henrich; Phys. Rev. B36 (1987) 3413.

[8] P. Liu, T. Kendelewicz, G.E. Brown, E.J. Nelson, and S.A. Chambers, Surf. Sci. 417 (1998) 53.

[9] J. Ahn and J.W. Rabalais, Surf. Sci. 388 (1997) 121.

[10] J.W. Elam, C.E. Nelson, M.A. Cameron, M.A. Tolbert, and S.M. George, J. Phys. Chem. B 102 (1998) 7008.

[11] R.M. Jaeger, J. Libuda, M. Bäumer, K. Homann, H. Kuhlenbeck, H.-J. Freund , J. Electron Spectrosc. Relat. Phenom. 64/65 (1993) 217.

[12] G. Zwicker and K. Jacobi, Surf. Sci. 131 (1983) 179.

[13] H.H. Kung, Transition Metal Oxides: Surface Chemistry and Catalysis, Studies in Surface Science and Catalysis 45, Elsevier Science, New York (1991).

[14] W. Weiss, D. Zscherpel and R. Schlögl; Catal. Lett. 52 (1998) 215.

[15] M.M. Khader, G.H. Vurens, I.-K. Kim, M. Salmeron, G.A. Somorjai, J. Am. Chem. Soc. 109 (1987) 3581.

[16] S. Blonski and S.H. Garofalini, J. Phys. Chem. 100 (1996) 2201.

[17] W. Ranke and W. Weiss, Surf. Sci. 414 (1998) 238.

[18] Y. Joseph, W. Ranke, W. Weiss, submitted to J. Phys. Chem.

[19] M.P. Seah and W.A. Dench, Surf. Interface Analysis 1 (1979) 2.

[20] W. Weiss, M. Ritter, D. Zscherpel, M. Swoboda and R. Schlögl; J. Vac. Sci. & Technol. A16 (1998) 21.

[21] D.E. Brown, S.M. George, C. Huang, E.K.L. Wong, K.B. Rider, R.S. Smith, B.D. Kay, J. Phys. Chem. 100 (1996) 4988.

[22] W. Weiss and M. Ritter, Phys. Rev. B 59 (1999) 5201.

[23] H.C. Galloway, P. Sautet and M. Salmeron; Phys. Rev. B 54 (1996) R11145.

[24] Y.J. Kim, C. Westphal, R.X. Ynzunza, H.C. Galloway, M. Salmeron, M.A. Van Hove and C.S. Fadley; Phys. Rev. B55 (1997) R13448 .

[25] Th. Schedel-Niedrig, W. Weiss and R. Schlögl; Phys. Rev. B 52 (1995) 17449.

[26] W. Ranke, M. Ritter and W. Weiss, Phys. Rev. B60 (1999) 1527.

[27] M. Ritter and W. Weiss; Surf. Sci. 432 (1999) 81.

[28] Sh.K. Shaikhutdinov, M. Ritter, X.-G. Wang, H. Over, W. Weiss, Phys. Rev. B (1999) in press.

[29] D.W. Turner, A.D. Baker, C. Baker, and C.R. Brundle; Molecular Photoelectron Spectroscopy (Wiley-Interscience, New York 1970).

[30] D. Schmeisser, F.J. Himpsel, G. Hollinger, B. Reihl, and K. Jacobi, Phys. Rev. B27 (1983) 3279.

[31] S. Katsumata and D.R. Lloyd , Chem. Phys. Lett. 45 (1977) 519.

[32] X.D. Peng and M.A. Barteau; Surface Science 233 (1990) 283.

[33] H. Ogasawara, J. Yoshinobu, M. Kawai, Chem. Phys. Lett. 231 (1994) 188.

[34] J. Isrealachvili and H. Wennerström, Nature 379 (1996) 219.

[35] L. Giordano, J. Goniakowski and J. Suzanne, Phys. Rev. Lett. 81 (1998) 1271.